

Original Article

Open Access



Concentration distribution and group disparity of traffic-derived NO₂ exposure in Baoshan District

Xiao Luo¹, Siqi Wang¹, Chao Liu², Qingyan Fu³, Huizi Wang¹, Min Yi³, Xi Guo⁴, Qian Wang⁵, Yangjing Fu¹

¹College of Transportation Engineering, Tongji University, Shanghai 201804, China.

²College of Architecture and Urban Planning, Tongji University, Shanghai 200092, China.

³State Environmental Protection Key Laboratory of Formation and Prevention of Urban Air Pollution Complex, Shanghai Academy of Environmental Sciences, Shanghai 200233, China.

⁴School of Computer and Communication Engineering, University of Science and Technology Beijing, Beijing 100083, China.

⁵Shenzhen Urban Transport Planning Center CO., LTD, Shenzhen 518057, Guangdong, China.

Correspondence to: Qian Wang, Shenzhen Urban Transport Planning Center CO., LTD, Intersection of Hongmu 1st Street and Hongmu 3rd Street, Longhua District, Shenzhen 518057, Guangdong, China. E-mail: wangqian@sutpc.com; Yangjing Fu, College of Transportation Engineering, Tongji University, No. 4800, Cao'an Road, Jiading District, Shanghai 201804, China. E-mail: 2331723@tongji.edu.cn

How to cite this article: Luo, X.; Wang, S.; Liu, C.; Fu, Q.; Wang, H.; Yi, M.; Guo, X.; Wang, Q.; Fu, Y. Concentration distribution and group disparity of traffic-derived NO₂ exposure in Baoshan District. *Carbon Footprints* 2025, 4, 14. <https://dx.doi.org/10.20517/cf.2024.53>

Received: 3 Dec 2024 **First Decision:** 18 Mar 2025 **Revised:** 16 Apr 2025 **Accepted:** 13 May 2025 **Published:** 21 May 2025

Academic Editor: Yuli Shan **Copy Editor:** Fangling Lan **Production Editor:** Fangling Lan

Abstract

Motor vehicles are a major source of NO₂ emissions, making traffic-related pollution a key target for urban air pollution control management. However, research on traffic-related NO₂ exposure risks in China remains nascent, particularly regarding spatio-temporal variations and exposure inequities. To support evidence-based public health policies, it is essential to investigate group disparities in exposure across both spatial and temporal dimensions. This study utilizes the CALPUFF model and mobile phone signal data to examine the spatio-temporal patterns and population group disparities in NO₂ exposure within Baoshan District, Shanghai, China. The findings reveal a bimodal diurnal pattern, with higher NO₂ exposure levels on weekdays and lower levels on weekends. Areas with heavy traffic and high population density, such as port zones and the outer ring expressway, are identified as the most vulnerable. Furthermore, males and younger age groups experience greater exposure to traffic-related NO₂, whereas elderly individuals are comparatively less exposed.

Keywords: CALPUFF model, pollution modeling, spatio-temporal variation, NO₂ exposure risk, environmental justice



© The Author(s) 2025. **Open Access** This article is licensed under a Creative Commons Attribution 4.0 International License (<https://creativecommons.org/licenses/by/4.0/>), which permits unrestricted use, sharing, adaptation, distribution and reproduction in any medium or format, for any purpose, even commercially, as long as you give appropriate credit to the original author(s) and the source, provide a link to the Creative Commons license, and indicate if changes were made.



INTRODUCTION

Nitrogen dioxide (NO₂), a primary contributor to atmospheric acid deposition, photochemical smog, and other pollution issues, has increasingly become a key focus of air pollution control efforts. While emissions from industrial and domestic sources have steadily declined over time, those from transportation and other mobile sources have increased, reaching 6.336 million tons and accounting for over 51.3% of total NO₂ emissions^[1]. In urban areas, motor vehicles are a major source of NO₂ pollution. Several studies have confirmed that short-term exposure to NO₂ can result in airway hyperresponsiveness and impaired lung function, while long-term exposure may compromise immunity and heighten the risk of respiratory infections^[2]. With rapid urbanization, NO₂ pollution from road traffic is expected to rise, posing greater and more widespread risks to public health.

Exposure levels are influenced by both pollutant concentrations in the areas individuals occupy and the duration of time spent in those locations^[3,4]. Thus, exposure is determined by the spatial and temporal distribution of both air pollutants and population presence. However, research on traffic-related exposure risk in China remains in its early stages, particularly regarding environmental justice. It remains unclear whether vulnerable groups are disproportionately affected or how such disparities evolve over time and space.

To address this gap, we propose an evaluation framework to assess the exposure risk from traffic-derived NO₂ pollution, using Shanghai's Baoshan District as a case study. Beyond pollution simulation, this study makes two additional contributions to the pollution modeling literature. First, it introduces a novel approach that integrates the CALPUFF atmospheric dispersion model with high-resolution mobile phone signaling data, enabling a dynamic exposure risk assessment that accounts for real-time human mobility patterns. The fine spatio-temporal resolution of these data allows for more accurate identification of vulnerable groups, especially during peak traffic hours and in high-emission zones, thereby significantly improving the accuracy and realism of exposure assessments. Second, from an environmental justice perspective, we investigate disparities in exposure across gender and age groups using time-resolved, activity-based population data rather than static census data. This approach uncovers hidden inequalities in traffic-related NO₂ exposure that are often overlooked in traditional studies. Notably, this research pioneers the application of dynamic exposure modeling to assess intra-urban exposure inequities within a Chinese context, a topic that remains underexplored in current literature. Our findings provide both empirical evidence and methodological advancement that support the development of equity-oriented, fine-grained traffic pollution mitigation policies in rapidly urbanizing regions.

BACKGROUND

Application of the CALPUFF model

In current environmental impact assessments and air pollutant dispersion simulation studies, small- to medium-scale air quality models are widely applied in scenarios such as industrial emissions and urban pollution control. Commonly used models include AERMOD, ADMS (Atmospheric Dispersion Modelling System), and CALPUFF. Among these, AERMOD, a steady-state Gaussian model recommended by the U.S. Environmental Protection Agency (EPA), is extensively employed to simulate pollutant dispersion over short ranges and relatively flat terrains^[5,6]. Its advantages include a well-established framework, computational efficiency, and ease of integration with meteorological data. However, AERMOD performs poorly under conditions of low wind speeds, complex topography, or non-steady-state atmospheric dynamics. ADMS, developed by the UK's Cambridge Environmental Research Consultants (CERC), is also a steady-state model but features pollutant chemistry compared to AERMOD, demonstrating superior performance in urban micro-meteorological environments^[7]. Nevertheless, ADMS is less suitable for long-

range transport modeling and often incurs higher costs due to commercial licensing requirements.

In contrast, CALPUFF employs a non-steady-state Lagrangian puff modeling approach, enabling dynamic simulation of pollutant dispersion under changing wind directions and speeds. This makes it particularly suited for simulating long-distance transport, complex terrains, and coastal or land-sea interface pollution scenarios^[8]. The model supports time-varying emission sources, dynamic meteorological inputs, and integration with diverse meteorological models^[9], thereby enabling high-resolution spatiotemporal simulations. With its non-steady-state modeling capability and flexible input mechanisms, CALPUFF exhibits strong adaptability and accuracy, positioning it as one of the most promising tools for simulating complex pollution dispersion scenarios.

In the transportation sector, CALPUFF has been widely applied in four key areas: (1) spatiotemporal simulation of air pollution; (2) assessment of exposure risks to traffic-related pollutants; (3) investigation into emission inventories; and (4) analysis of traffic impact scenarios.

Regarding spatiotemporal simulation, research primarily targets pollutants closely associated with vehicular emissions, including nitrogen oxides (NO_x)^[10,11], carbon monoxide (CO)^[12], carbon dioxide (CO₂)^[13], sulfur dioxide (SO₂)^[14], and particulate matter (PM)^[15,16]. Most studies examine the spatial and temporal distribution characteristics of two or three types of pollutants simultaneously.

For assessing exposure risks, a study in the Montreal region of Canada employed a four-stage traffic model, an emissions model, and CALPUFF to quantify the total emissions associated with residents' daily travel. The findings revealed that exposure risk increases significantly during outdoor activities, with average outdoor exposure levels 23%-44% higher than those indoors, regardless of indoor air quality conditions^[17]. These results underscore the importance of incorporating travel trajectory data when evaluating individual exposure risks.

In the context of emission inventory development and traffic scenario analysis, it is crucial to allocate responsibility for emissions and formulate targeted mitigation strategies. The Montreal case study revealed that improving vehicle performance yields more substantial reductions in traffic-related pollution than investments in public transportation or other policy interventions^[17].

Air pollution exposure assessment

Accurate assessment of air pollution exposure requires not only high-resolution measurements of pollutant concentrations but also a comprehensive understanding of human activity patterns^[18]. Previous studies have largely focused on static population data, such as census statistics^[19,20] and nighttime light imagery^[21,22]. At the macro-static level, exposure risk is typically evaluated using indicators such as air quality concentration^[23], population exposure intensity^[24], and population-weighted exposure level (PWEL)^[25]. However, air quality concentration alone does not account for the spatial heterogeneity of population distribution and has been criticized for its theoretical limitations^[26]. Population exposure intensity is highly sensitive to population density, and substantial regional differences can lead to polarized exposure risk assessments. By comparison, PWEL is capable of capturing fine-scale spatial variations in exposure risk and is widely used in urban-level studies in China^[27].

To overcome the limitations of macro-static assessments that overlook individual mobility, recent studies have incorporated dynamic population distribution data, such as travel surveys^[28,29] and mobile phone signal data^[30,31], to analyze exposure during various daily activities. For example, Guo *et al.* used mobile phone

signal data to examine spatial and temporal variations in $PM_{2.5}$ exposure risk among different socioeconomic groups in Shenzhen^[32]. Additionally, studies investigating exposure during commuting have revealed that traffic congestion and longer commuting distances significantly increase pollution exposure levels^[33].

Exposure equity and environmental justice

The principle of environmental justice asserts that all individuals, regardless of socioeconomic status, should have equitable access to public resources and share an equal burden of the health impacts resulting from environmental degradation^[34]. Originating in the United States in the 1980s, the concept initially focused on the spatial inequities associated with the placement of polluting facilities in marginalized communities, exemplified by the 1,982 protests against the siting of a hazardous waste landfill in Warren County, North Carolina^[35]. Over time, this framework has expanded to encompass disparities in air quality, access to transportation, flood risk management, and other dimensions, evolving into a critical interdisciplinary field that bridges social geography and public health.

A major subfield of environmental justice research is the assessment of equity in air pollution exposure, which seeks to identify disparities in exposure levels among different sociodemographic groups (e.g., by gender, age, income, ethnicity). Extensive evidence confirms that low-income and less-educated populations, along with children, the elderly, and ethnic minorities, often bear a disproportionate share of pollution exposure risks^[36]. For example, studies in the United Kingdom have revealed a “Matthew effect” in air quality improvement policies, whereby middle- to high-income groups - who typically have lower baseline exposure - benefit disproportionately, while high-exposure, impoverished communities suffer unintended consequences during policy transitions. This trend risks deepening regional resource allocation conflicts and perpetuating environmental injustices.

However, current research on exposure equity is largely concentrated in developed nations, particularly the United States and the United Kingdom, with relatively limited attention to developing countries such as China. Amid China’s rapid urbanization and industrialization, air pollution from transportation, ports, and construction has become increasingly intertwined with daily human activity, intensifying exposure disparities across social groups. Consequently, examining group-specific disparities in traffic-related pollution exposure in Chinese cities is now a critical pathway for promoting health equity and enhancing environmental governance.

METHODS

Case study

Baoshan District, located in the northeastern part of Shanghai, falls under the city’s jurisdiction. Positioned at the confluence of the Yangtze River, Huangpu River, and Yunzaobang, the district features a 46.5-kilometer-long shoreline. Its port area connects to more than 400 ports across 164 countries and regions. As a key “waterway gateway” for Shanghai, Baoshan features an integrated transport infrastructure that links waterborne shipping with highways, railways, and urban roads [Figure 1]. Due to the area’s distinctive industrial profile, a high concentration of warehousing and logistics enterprises has developed, resulting in frequent freight vehicle activity. Consequently, traffic-related air pollution in this district is notably severe.

Simulation of traffic-derived NO_x pollution using the CALPUFF model

The CALPUFF modeling system consists of four main components: a preprocessing module, a meteorological module (CALMET), a dispersion module (CALPUFF), and a postprocessing module (CALPOST) [Figure 2]. First, the preprocessing module converts land use and terrain elevation data into georeferenced formats compatible with the CALMET module. It also processes surface and upper-air



Figure 1. Road network in the study area.

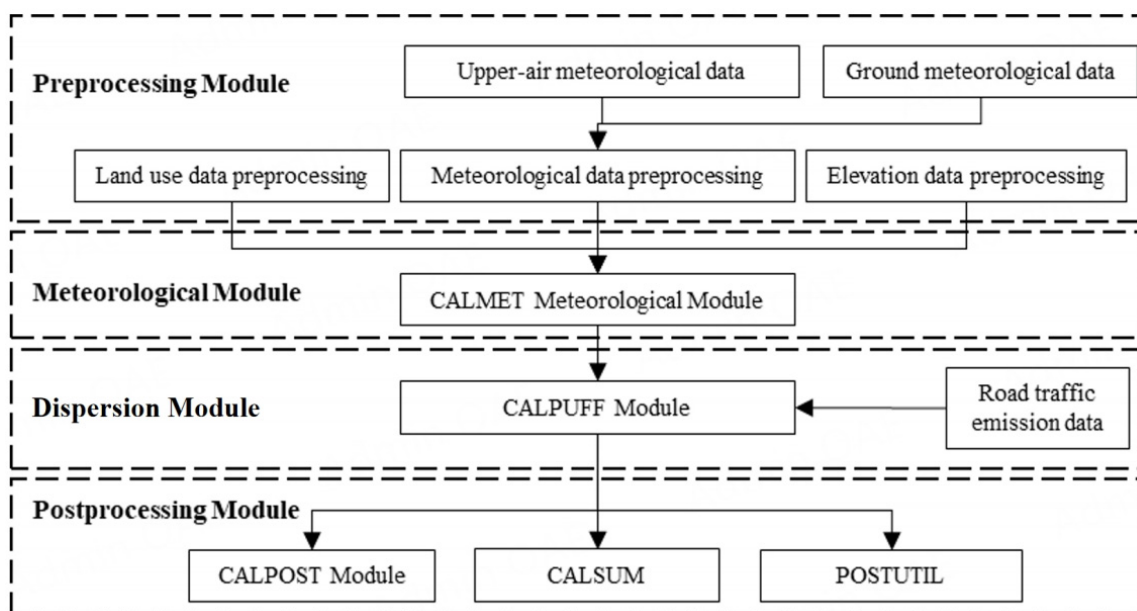


Figure 2. Framework of the CALPUFF model.

meteorological data. Next, CALMET generates hourly, three-dimensional diagnostic fields of wind and temperature, which characterize the local geographic and meteorological conditions. Then, the CALPUFF module simulates the atmospheric dispersion of pollutants by generating air pollutant puffs and modeling their physical transport and chemical transformation in the atmosphere. Finally, the resulting concentration data are input into the CALPOST module, which produces geographic information output files suitable for statistical analysis and ArcGIS mapping.

The CALPUFF model utilizes a three-dimensional grid system, where the X, Y, and Z axes represent the east-west, north-south, and vertical directions, respectively. In this study, the Universal Transverse Mercator (UTM) coordinate system is adopted as the projection system, with the World Geodetic System 1984 (WGS-84) serving as the geodetic datum.

The study area encompasses a 25×27 km region centered on Baoshan District. The UTM coordinates of the origin are (337.160, 3459.74) km, and the horizontal grid resolution is set to 0.5 km. The domain consists of 50 grid points along the X-axis (east-west) and 54 grid points along the Y-axis (north-south). Vertically, the Z-axis includes 11 levels with top heights defined as 0, 20, 40, 80, 160, 320, 640, 1,200, 2,000, 3,000, and 4,000 m.

Terrain elevation data are sourced from the USGS SRTM1 dataset. In the terrain preprocessing module, these data are converted into the “terrel.dat” file to represent the elevation of each grid cell. Land use data are derived from the USGS Global Land Cover Characteristics (GLCC) database, specifically the Asian region (USGS Global (Lambert Azimuthal) for Eurasia-Asia), with a spatial resolution of 1 km. These data are processed into the “lu.dat” file to describe land use across the grid.

Ground-level meteorological data are obtained from 11 observation stations across Shanghai, including Minhang, Baoshan, Jiading, Chongming, Xujiahui, Nanhui, Pudong, Jinshan, Qingpu, Songjiang, and Fengxian [Table 1]. The dataset spans from 00:00 on November 11 to 23:00 on November 30, 2019, and includes hourly records of wind speed (m/s), wind direction (degrees), temperature (Kelvin), cloud cover (tenths), cloud base height (hundreds of feet), surface pressure (hPa), and relative humidity (%). To maintain data continuity for model input, missing values in variables such as wind speed, temperature, or cloud cover were filled using linear interpolation based on the average of adjacent time points.

Upper-air meteorological data must include at least two observations per day, covering geopotential height, temperature, wind direction, and wind speed at the 500, 700, 850, 925, and 1000 hPa pressure levels. In this study, the data were sourced from publicly accessible datasets provided by the University of Wyoming (UWyo) and the National Oceanic and Atmospheric Administration (NOAA).

The road traffic emission data for Baoshan District [Table 2] were obtained from the Shanghai Environmental Monitoring Center. These data encompass all 4,511 major roads in the district and span the period from 00:00 on November 11 to 23:00 on November 30, 2019. The dataset includes information such as road identification number, date, time, vehicle type, road length, average vehicle speed, traffic flow, vehicle mileage, and NO_x emissions.

Conversion rate of NO_2/NO_x

Nitrogen oxide (NO_x) emissions are commonly used as a statistical metric for pollution source data. When air quality models are employed to simulate the spatial and temporal distribution of NO_2 concentrations, and photochemical models are unable to predict NO and NO_2 separately, NO_2 concentrations are typically

Table 1. Basic information of ground meteorological observation stations in Shanghai

Name	Station ID	X (km)	Y (km)	Observation site elevation (m)
Minhang	58361	344.16	3,442.17	5.5
Baoshan	58362	352.12	3,473.96	5.5
Jiading	58365	332.97	3,471.03	4.4
Chongming	58366	357.11	3,504.45	4.3
Xujiahui	58367	350.56	3,451.95	4.6
Nanhui	58369	384.38	3,436.49	5
Pudong	58370	360	3,456.02	4.4
Jinshan	58460	342.03	3,400.84	5.2
Qingpu	58461	320.97	3,445.99	4
Songjiang	58462	331.42	3,435.02	4.2
Fengxian	58463	356.19	3,418.08	4.6

Table 2. Road traffic emission data for Baoshan district

Field name	Explanation
Road ID	Unique identifier with no inherent meaning
Date	Format: "YY-MM-DD"
Time	Time unit: 1 h
Vehicle type	0: Total; 11: Taxi; 21: Bus; 31: Shanghai-plated small passenger car; 32: Out-of-province small passenger car; 33: Shanghai C-plated small passenger car; 41: Small truck; 51: Large bus; 61: Large truck; 71: Container truck
Road length	Unit: kilometers
Average vehicle speed	Average speed of all vehicle types passing through the road per hour, unit: kilometers/hour
Traffic flow	Number of vehicles passing through the road per hour, unit: vehicles/hour
Vehicle mileage	Total vehicle mileage per hour, unit: vehicle kilometers/hour
NO _x emissions	Total NO _x emissions from all vehicle types per hour, unit: grams/hour

estimated based on NO_x data. According to the Technical Guidelines for Environmental Impact Assessment - Atmospheric Environment, issued by the Ministry of Ecology and Environment of China, a conversion rate of 90% for NO₂/NO_x should be used when calculating hourly or daily mass concentrations of NO₂. For annual average mass concentrations, an estimated conversion rate of 75% is recommended^[37]. However, this standardized approach may constrain the flexibility of air pollution simulations, potentially leading to inaccurate assessments of ambient air quality. To improve this, Luo *et al.* proposed a proportional simulation method for converting NO_x to hourly NO₂ concentrations^[38]. This method derives the NO₂/NO_x conversion rate from hourly concentration data collected at meteorological observation stations. Results show that it more accurately and reasonably simulates the dispersion and transport of NO₂.

In this study, NO₂ concentrations are derived using an hourly NO₂/NO_x conversion rate. The data used to calculate the conversion rates were obtained from traffic monitoring stations in Shanghai, as shown in Table 3. These include five roadside air monitoring stations, one airport station, and two port stations, covering the period from 00:00 on November 11 to 23:00 on November 30, 2019. The five roadside monitoring stations are located within the Outer Ring Road, while the airport and port stations are also situated nearby.

The conversion rate calculation formula is as follows, where *i* represents the hour, NO_{2*i*} is the NO₂ concentration at hour *i*, and NO_{*x**i*} is the NO_x concentration at hour *i*:

$$\text{Conversion Rate } i = \text{NO}_{2i} / \text{NO}_{xi} \quad (1)$$

Table 3. Basic information on Shanghai traffic monitoring stations

Station name	Longitude	Latitude	Station type
Caoyi road roadside station	121.435	31.174	Roadside air station
Yan'an West road roadside station	121.414	31.318	Roadside air station
Gonghe new road roadside station	121.449	31.277	Roadside air station
Dongfang road roadside station	121.528	31.212	Roadside air station
National exhibition center	121.467	31.207	Roadside air station
Hongqiao airport station	121.352	31.208	Airport air station
Waigaoqiao port area - station 2	121.582	31.369	Port air station
Waigaoqiao port area - station 4	121.654	31.331	Port air station

Mobile phone signal data

The mobile phone signal dataset for Shanghai, covering the period from November 11 to November 30, 2019, was provided by JISMAART (<http://daas.smartsteps.com/>, accessed on January 19, 2021). This dataset includes information on time, location, and users. Initially, it comprised data on approximately 5.28 million mobile phone users, which can be considered representative of Shanghai's population of around 23.55 million, excluding the Chongming District^[39].

Using data from the Seventh National Population Census as a reference, SPSS 26.0 was employed to perform a correlation analysis and paired sample *t*-test to compare the spatial distribution, gender composition, and age structure of the resident population in Shanghai, as inferred from the mobile signaling data. These analyses aimed to verify whether significant differences exist between the two datasets and, in turn, to assess the extent to which mobile signaling data can represent the demographic distribution of Shanghai's resident population.

Regarding population distribution, the proportions of residents in each administrative district, as derived from both the census and the mobile signaling data, are presented in Table 4. The Pearson correlation coefficient was calculated at 0.998, indicating a strong linear relationship. Furthermore, the significance level of the paired sample *t*-test was 0.999, which is much greater than the conventional threshold of 0.05, suggesting that there is no statistically significant difference between the two datasets at the 0.05 level. Overall, these results confirm that mobile signaling data can reliably represent the population distribution across Shanghai's various districts.

In analyzing the gender structure, the gender ratio, defined as the number of males per 100 females, was used as the evaluation metric. Table 5 presents the gender ratios for each administrative district in Shanghai based on data from the Seventh National Population Census and mobile signaling data. The Pearson correlation coefficient between the two datasets was 0.794, indicating a strong positive correlation. The paired sample *t*-test result was 0.374, greater than the 0.05 significance level. This suggests there is no statistically significant difference in the mean gender ratios between the two datasets, supporting the conclusion that mobile signaling data can effectively represent gender structure across different districts in Shanghai.

Regarding age structure, a comparative analysis was conducted for three age groups (0-14, 15-64, and 65 years and older) across Shanghai's administrative districts, as shown in Table 6. The Pearson correlation coefficients for the three age groups are 0.518, 0.912, and 0.942, respectively - all above 0.5 - indicating

Table 4. Distribution of the resident population across different districts of Shanghai

District	Seventh national census data (%)	Mobile signaling data (%)	District	Seventh national census data (%)	Mobile signaling data (%)
Huangpu	2.73	2.14	Baoshan	9.22	9.42
Xuhui	4.59	3.79	Jiading	7.57	8.24
Changning	2.86	3.33	Pudong	23.44	25.66
Jing'an	4.03	3.8	Jinshan	3.4	2.46
Putuo	5.11	5.07	Songjiang	7.88	8.22
Hongkou	3.13	2.53	Qingpu	5.25	5.06
Yangpu	5.13	4.46	Fengxian	4.71	4.72
Minhang	10.95	11.1			

Data source: 2020 national population census.

Table 5. Gender structure in Shanghai's administrative districts

District	Seventh national census data	Mobile signaling data	District	Seventh national census data	Mobile signaling data
Huangpu	107.59	101.63	Baoshan	109.51	100.13
Xuhui	95.06	95.02	Jiading	116.83	114.4
Changning	90.91	98.5	Pudong	108.04	103.32
Jing'an	95.19	96.79	Jinshan	113.74	117.63
Putuo	97.14	101.68	Songjiang	114.7	107.42
Hongkou	97.17	96.43	Qingpu	120.39	120.64
Yangpu	97.91	103.05	Fengxian	116.78	117.26
Minhang	107.72	93.6			

Data source: 2020 national population census.

Table 6. Age structure in Shanghai's administrative districts

District	Seventh national census data			Mobile signaling data		
	0-14	15-65	≥ 65	0-14	15-65	≥ 65
Huangpu	8.67	72.84	18.48	8.74	73.72	17.54
Xuhui	9.79	69.6	20.61	9.39	71.48	19.13
Changning	8.89	70.46	20.65	9.11	71	19.89
Jing'an	9.31	68.72	21.97	10.78	70.2	19.02
Putuo	9.39	69.48	21.12	10.04	69.34	20.62
Hongkou	8.19	68.58	23.23	8.53	69.2	22.27
Yangpu	8.84	69.31	21.85	9.12	70.47	20.41
Minhang	10.86	75.11	14.02	9.57	76.91	13.52
Baoshan	10.01	74.61	15.39	8.54	74.72	16.74
Jiading	9.81	78.12	12.07	9.62	77.39	12.99
Pudong	10.48	74.53	14.99	10.03	76.32	13.65
Jinshan	9.22	73.75	17.03	9.54	70.75	19.71
Songjiang	10.7	78.39	10.91	10.76	76.87	12.37
Qingpu	8.86	79.58	11.56	9.31	76.79	12.9
Fengxian	9.28	76.96	13.76	9.21	77.92	12.87

Data source: 2020 national population census.

strong correlations. The paired sample *t*-test results are 0.997, 0.627, and 0.499, all exceeding the 0.05 significance threshold. These results suggest that there are no significant differences in the age structure of the three groups, confirming that mobile signaling data can reliably reflect the age structure of different regions in Shanghai.

Traffic-derived NO₂ pollution exposure assessment

This study adopted the population-weighted exposure level (PWEL) as the indicator for assessing exposure to traffic-derived NO₂ pollution, as proposed by Fu and Kan^[25]. PWEL was calculated by combining predicted NO₂ concentrations with dynamic population distribution data. The CALPUFF model was used to estimate NO₂ concentrations for each standardized 1,000 × 1,000 m grid across different time periods. Hourly gridded population data were obtained from mobile phone records. PWEL was then used to evaluate the risk of exposure to traffic-derived NO₂ pollution in each grid over various time intervals. The formula is as follows:

$$E_i = (P_i \times C_i) / \sum_{i=1}^n P_i \quad (2)$$

where *i* denotes the grid index, *n* is the total number of grids, *E_i* represents the potential population exposure in grid *i*, *P_i* is the population of grid *i* during a certain period, and *C_i* is the NO₂ concentration in grid *i*. The overall population-weighted exposure level of traffic-derived NO₂ pollution in Shanghai was assessed using Formula (3), where *E* represents the total potential exposure across the city:

$$E = \sum_{i=1}^n E_i \quad (3)$$

RESULTS

Temporal variation in the NO₂/NO_x conversion rate in Shanghai

The NO₂/NO_x conversion rate in Shanghai predominantly falls within the range of 0.3–0.7 [Figure 3], which is comparable to the range reported in Seoul (0.4–0.8)^[38]. However, it significantly deviates from the value suggested by China's Ministry of Ecology and Environment, as previously mentioned. Therefore, estimating NO₂ concentrations using hourly data from air quality monitoring stations and a ratio-based hourly simulation method is crucial for accurately modeling the temporal and spatial distribution of NO₂ exposure risk.

Spatiotemporal distribution of traffic-related NO₂

There is significant spatiotemporal variability in NO₂ concentrations related to road traffic. Temporally, NO₂ concentrations exhibit a “bimodal” distribution that aligns with the typical daily traffic pattern: the highest concentrations occur during morning and evening rush hours, reaching 15.51 and 18.36 µg/m³, respectively. Concentrations are slightly lower during the daytime, averaging around 12.62 µg/m³, and drop to their lowest levels at night, averaging just 7.12 µg/m³.

Spatially, NO₂ concentrations tend to decrease from the center of the road outward to both sides. Overall, higher concentrations are observed along major roadways, including the east-west Shanghai Ring Expressway (G1503) and Outer Ring Expressway (S20), as well as the north-south Hutai Road and Yunchuan Road. Elevated concentrations are also found near warehousing and logistics hubs, such as Baoyang Road at the confluence of two rivers. Furthermore, areas prone to frequent traffic congestion, such as expressway toll stations, entrance and exit ramps, and overpasses, exhibit higher pollutant levels compared to other road segments [Figure 4].

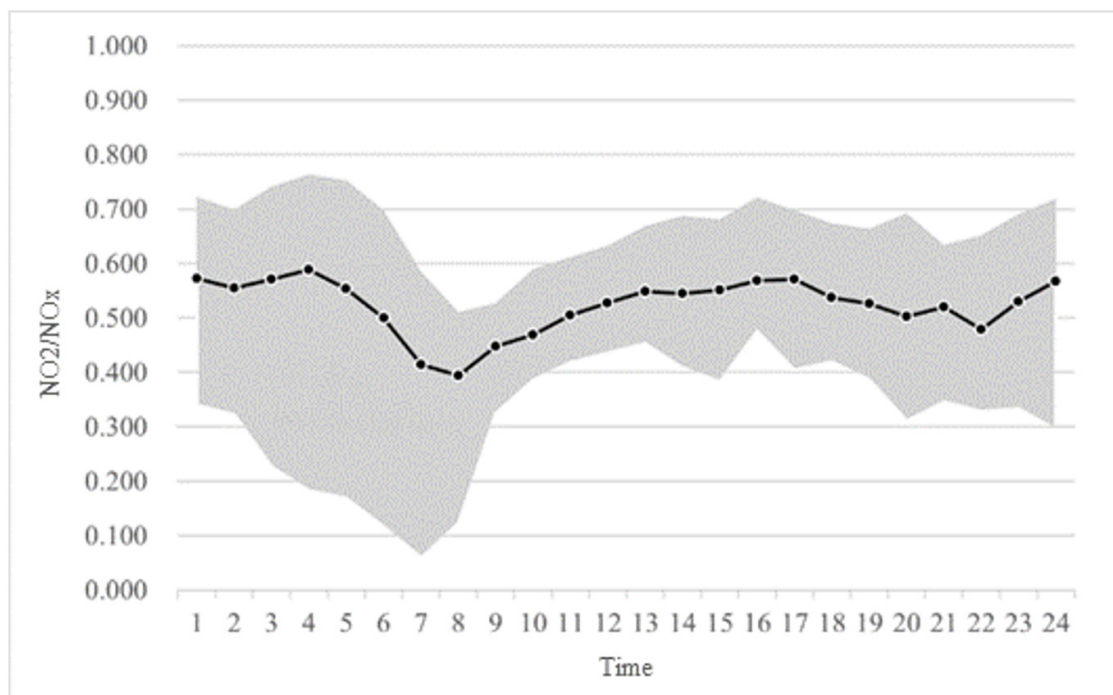


Figure 3. Temporal variation in the NO_2/NO_x conversion rate in Shanghai. (The broken line represents the mean hourly NO_2/NO_x conversion rate, and the grey shading area indicates the full range of hourly values).

Disparities in exposure and inequality

Wang *et al.* explored disparities in air pollution exposure and inequality from three aspects: temporal variation, spatial variation, and group disparity^[39]. Building on their framework, this paper integrates all three dimensions, with a particular focus on examining the underlying factors that influence the impact of traffic-derived NO_2 pollution on vulnerable populations.

Temporal variation

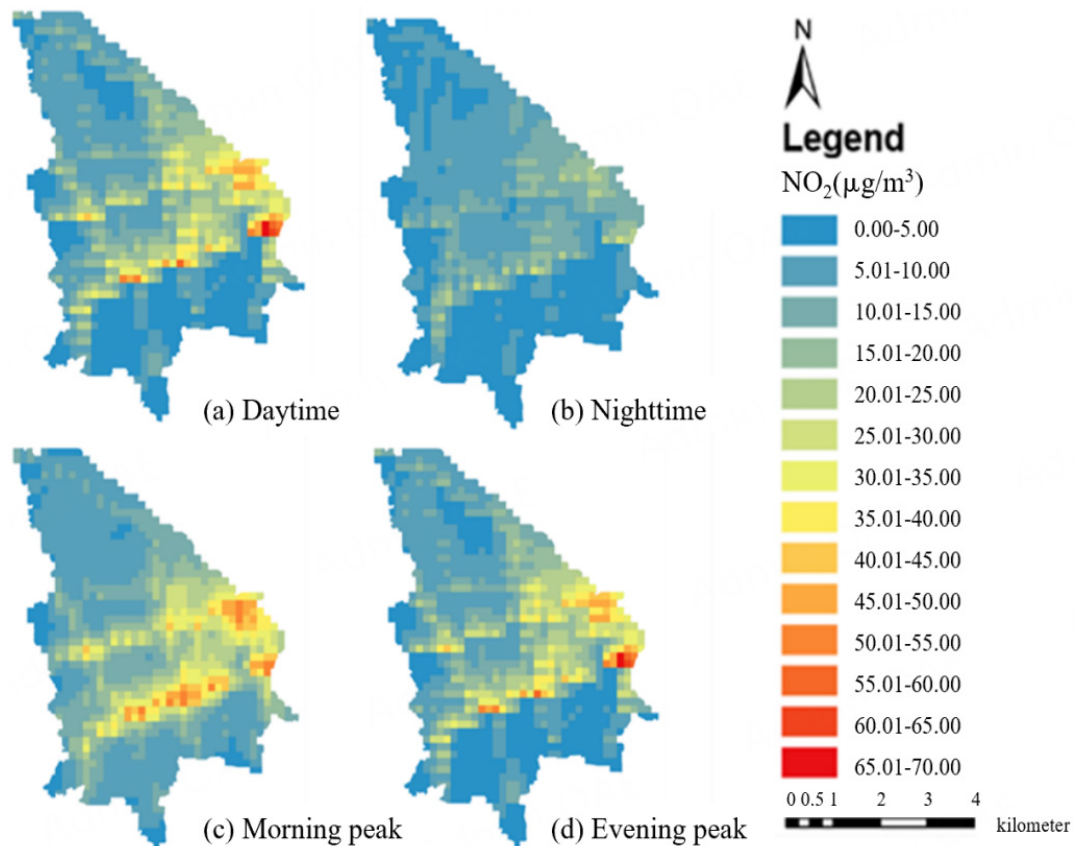
Exposure to traffic-related NO_2 pollution peaks during rush hours, with the highest levels occurring in the evening, followed by the morning rush, daytime, and the lowest levels at night. Compared to other time periods, the evening peak displays a greater variability in exposure levels [Table 7]. This suggests that the degree to which permanent residents of Baoshan District are affected by traffic pollution during this period varies significantly, resulting in unequal levels of environmental exposure within residential areas.

This study postulates that such disparities are associated with the travel behavior typical of the evening peak. This period is characterized by more dispersed travel times, a higher proportion of non-commuting trips, and greater diversity in travel patterns. In contrast to relatively uniform commuting routines of the morning rush, the evening rush reveals substantial heterogeneity in individuals' exposure to traffic-derived NO_2 pollution.

In terms of daily variation, exposure is higher on weekdays than on weekends [Figure 5]. This is primarily due to rigid weekday travel patterns driven by work and school schedules, resulting in dense traffic, frequent vehicle use, and elevated emissions. Consequently, residents are often forced to travel through heavily

Table 7. Summary statistics of traffic-derived NO₂ pollution exposure (μg/m³)

Period	Mean	Minimum	Maximum	Standard deviation
Daytime	12.62	12.31	12.75	0.15
Nighttime	6.62	6.58	6.67	0.02
Morning peak	16.00	15.83	16.14	0.10
Evening peak	18.41	18.13	18.63	0.15

**Figure 4.** Spatiotemporal simulation results of road traffic-related NO₂.

polluted areas. On weekends, travel tends to be more flexible and discretionary, with a reduction in travel frequency and lower concentrations of traffic-related NO₂ pollution, thereby decreasing exposure risk. However, this weekday-weekend distinction is less evident at night due to the continued operation of freight and logistics services. Nighttime travel tends to be limited in scope, and there is no significant variation in pollution exposure between weekdays and weekends, leading to a relatively stable risk level.

Spatial variation

In this study, the mean-standard deviation classification method is employed to depict the spatial distribution characteristics of traffic-derived NO₂ pollution exposure risk, with an emphasis on identifying areas with extreme exposure values. The mean exposure level serves as a baseline, and each grid is classified into one of four risk levels: low risk (0.5 and ≤ 1.5 SD), high risk (> 1.5 and ≤ 2.5 SD), and critical risk (> 2.5 SD).

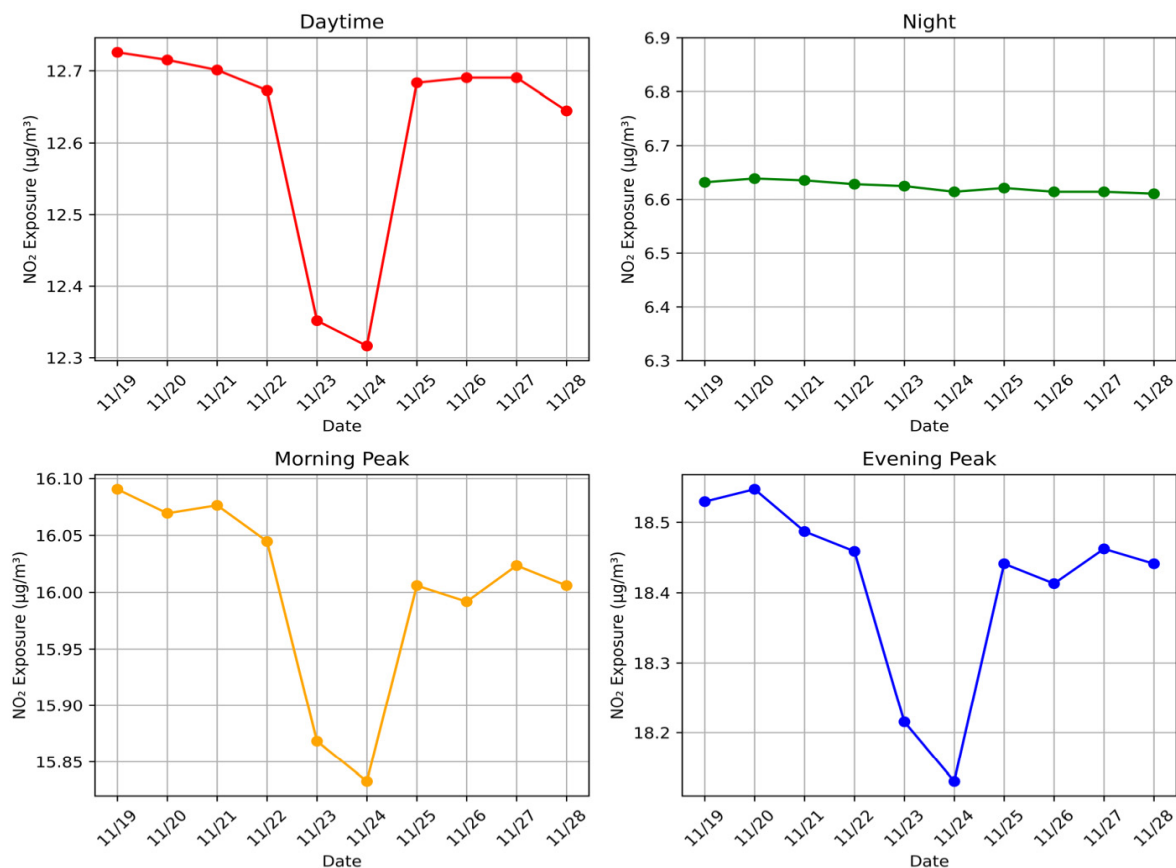


Figure 5. Time variation in traffic-derived NO₂ pollution exposure risk.

Areas with high traffic pollution exposure are concentrated in the southern part of Baoshan District, specifically including Wusong Street and Baoshan Town near Wusong Port, Gucun Town near Baoan Road-Hutai Road, and Yanghang Town near the Yunchuan Road overpass on the Outer Ring Road [Figure 6]. These locations are not only densely populated but are also surrounded by major arterial roads that function as the main external passages for Baoshan District, making them particularly vulnerable to disruption by transit traffic.

Group disparity

To investigate group disparity, user attribute information, including gender and age, was extracted from mobile phone signal data. Age was categorized into four groups: juvenile (≤ 18 years), young adults (19–44 years), middle-aged adults (45–64 years), and elderly (≥ 65 years).

Gender

Overall, males experienced a higher risk of exposure to traffic-derived NO₂ pollution compared to females [Figure 7]. The gender disparity in exposure was most evident during peak hours, when the average NO₂ exposure risk for males reached 0.76 µg/m³, approximately 4.59% higher than that of females. During the daytime hours, the exposure risk for males was around 0.61 µg/m³, about 6.20% higher than that of females. The lowest disparity occurred at night, with a male exposure level of 0.40 µg/m³, approximately 9.53% higher than that of females.

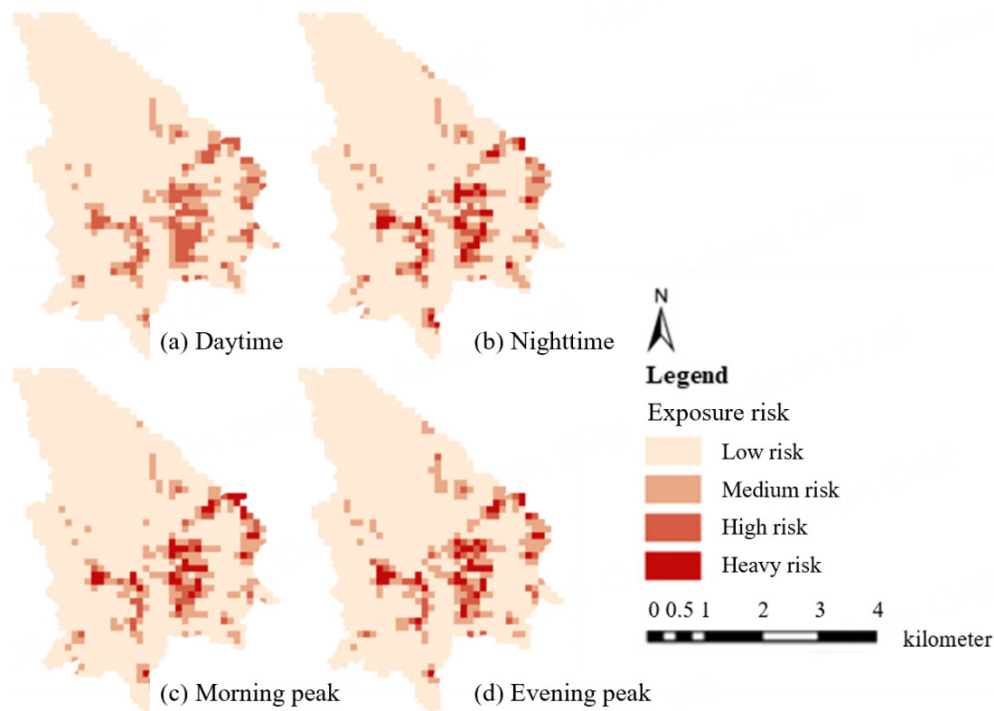


Figure 6. Spatial variation in traffic-derived NO₂ pollution exposure risk.

In Baoshan District, heavy industries such as steel smelting and port cargo handling are predominantly male-dominated. These occupations typically require early-morning start times and late-evening finishes, coinciding with urban traffic peak hours. During the morning commute, male workers traveling to industrial sites are exposed to elevated NO₂ concentrations due to the simultaneous start of industrial productions and increased freight vehicle activity in industrial zones. Consequently, significant pollution exposure occurs both en route and within the workplace. Similarly, at the end of the workday, another surge in pollution levels occurs in industrial districts and surrounding roadways, leading to additional NO₂ exposure for male workers. In contrast, female employment in such high-exposure industries is relatively low, contributing to their lower pollution exposure.

Male commuters are more inclined to drive private vehicles or use company-operated shuttles along expressways and arterial roads^[40]. During rush-hour congestion, these drivers are immersed in environments with elevated vehicular exhaust emissions, where NO₂ concentrations are significantly higher than during off-peak hours. Additionally, male commuters typically have longer commuting distances and durations, leading to greater cumulative inhalation of air pollutants. By contrast, female commuters more often use public transportation, such as subways, which are electrically powered and primarily operate underground, thereby minimizing direct exposure to surface-level vehicle emissions. Shorter travel distances further limit exposure duration for female commuters. Thus, even during the same peak-hour periods, differences in commuting patterns and distance contribute to higher NO₂ exposure among male commuters.

Beyond commuting, occupational and lifestyle differences further intensify gender disparities in pollution exposure during high-risk periods. Men are more likely to engage in occupations necessitating substantial outdoor or road-based activities - such as logistics, taxi driving, and express delivery - which typically peak

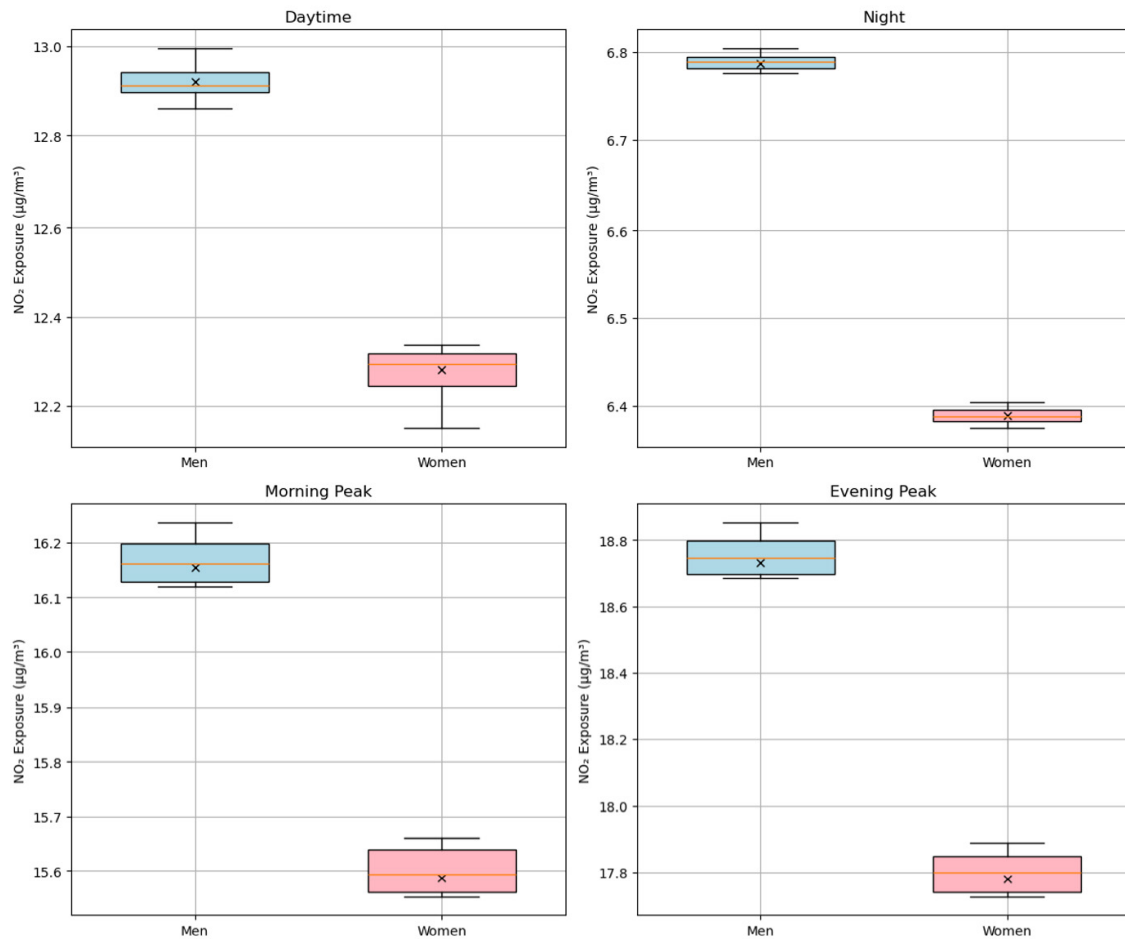


Figure 7. Gender-specific assessment of exposure risk to traffic-derived NO₂ pollution.

during morning and evening rush hours. These jobs inherently involve prolonged exposure to ambient air pollution at times when urban air quality is most deteriorated. In contrast, a greater proportion of women are employed in indoor settings or benefit from flexible work schedules, enabling some to avoid peak commuting times altogether, particularly due to family caregiving responsibilities. As a result, the differences in daily activity patterns between men and women substantially contribute to the observed disparities in cumulative NO₂ exposure.

Age

Different age groups exhibit varying levels of susceptibility to traffic-related NO₂ pollution, with the elderly experiencing the lowest exposure risk. Specifically, recorded exposure concentrations during different time periods were 10.58, 5.51, 14.67, and 15.78 µg/m³, respectively [Figure 8].

The observed disparities in NO₂ exposure across age groups are primarily attributable to differences in travel behavior. Working-age adults are frequently present in traffic environments during peak periods, when vehicular emissions are most intense. In contrast, older adults typically avoid peak-hour travel or remain within residential areas. Motor vehicle emissions are a major contributor to urban NO₂ pollution, accounting for over 40% of total nitrogen oxide emissions in Shanghai^[41]. Consequently, the substantial

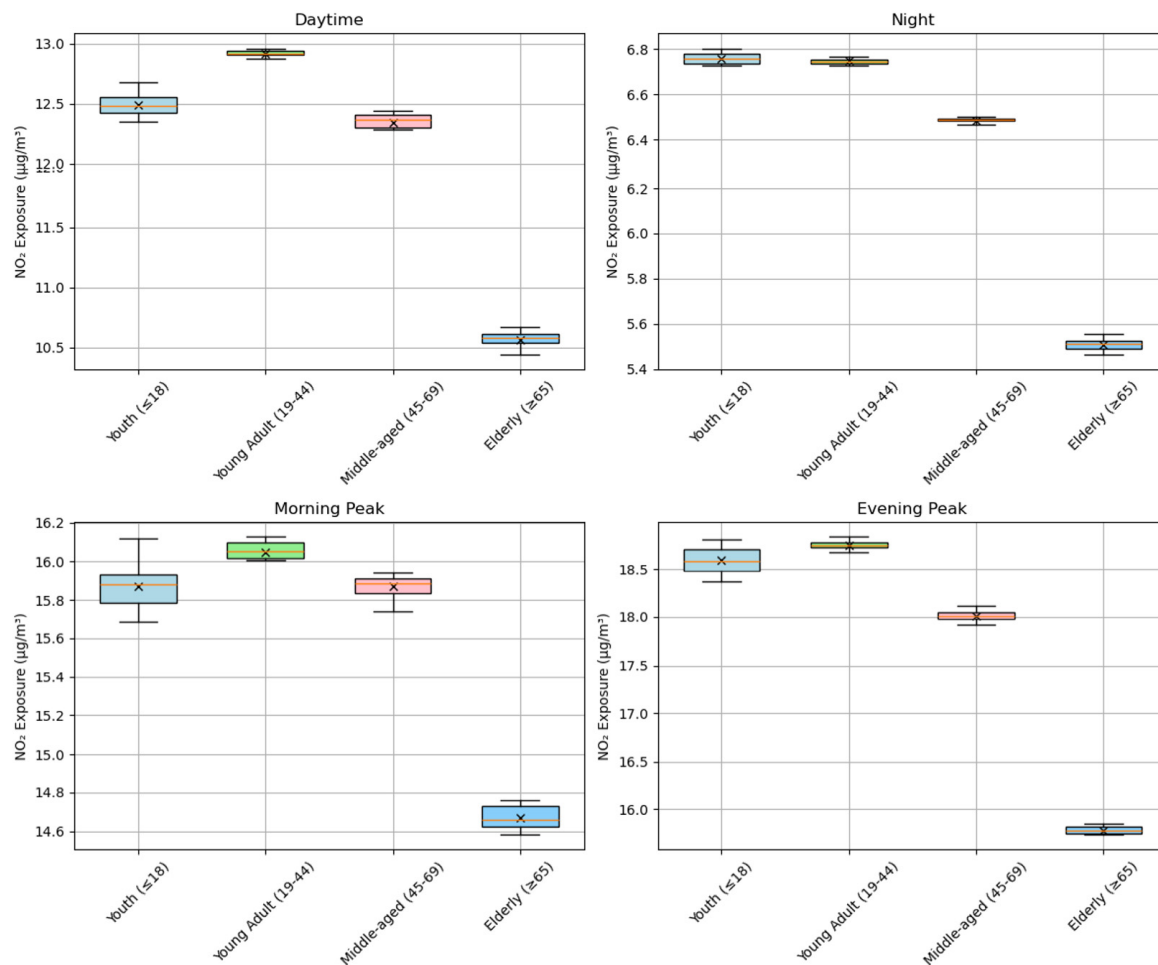


Figure 8. Age-specific risk assessment of exposure to road traffic-derived NO₂ pollution.

volume of NO_x generated by commuter traffic significantly elevates ambient NO₂ concentrations during rush hours. Individuals who commute during these high-exposure windows - mainly young and middle-aged adults - therefore experience markedly higher levels of NO₂ inhalation.

On the other hand, older adults and retired middle-aged individuals, whose activities are largely limited to indoor or community spaces^[42], benefit from the shielding effects of buildings and the attenuation of pollutants over distance, resulting in significantly lower exposure levels compared to individuals in close proximity to traffic corridors. Although office workers spend much of the day indoors, their cumulative NO₂ exposure is substantially increased by elevated concentrations during commuting periods. Adolescents, while spending most school hours indoors, still experience brief but significant exposure during travel to and from school. Thus, variations in daily activity patterns and mobility rhythms among age groups play a critical role in shaping the total NO₂ exposure accumulated throughout the day.

Comparative analysis

This study finds a high level of consistency with existing literature regarding the weekend effect on NO₂ pollution and the exposure characteristics of the elderly population. Regarding the weekend effect, Pommier (2023)^[43] demonstrated that NO_x emissions in UK cities were 1.54 to 3.05 times higher on weekdays than on weekends. Similarly, Demetillo *et al.* (2021)^[44], based on TROPOMI data, confirmed a significant decrease in

NO₂ concentrations in US cities on weekends, largely due to reduced heavy-duty diesel vehicle activity. These findings align with the weekend effect observed in this study. Together, the studies suggest that traffic emissions, particularly from freight transport and commuting, are the main contributors to elevated weekday NO₂ levels.

Concerning gender differences, the findings align with Mo *et al.* (2023), who found that men face higher NO₂ exposure risks due to occupational factors (e.g., transportation and outdoor work) and longer durations of outdoor activity, based on a Chinese cohort study^[45]. Hu *et al.* (2020) reported similar results in a multi-province survey across China^[46]. However, this contrasts with the findings of Kim *et al.* (2019) in South Korea, which indicated that women experienced significantly higher average NO₂ exposure than men (30.11 vs. 25.83 µg/m³), potentially due to indoor environmental exposures such as cooking fuel pollution^[47]. Furthermore, Chau *et al.* (2002) in Hong Kong noted that long-distance commuters (typically male) are overexposed, but also suggested that women might encounter different exposure pathways related to residential environments or domestic responsibilities^[48]. In addition, Setton *et al.* (2010), in a simulation study, found no gender differences at all, highlighting how exposure assessment methods (e.g., variations in spatial-temporal resolution between satellite data and individual monitoring) and differences in pollution source structures (traffic-dominant versus mixed-source cities) may influence observed outcomes^[49].

The finding that elderly individuals experience lower NO₂ exposure is consistent with most literature. Mo *et al.* (2023), in a national cohort study, found that older individuals are less exposed to high NO₂ concentrations along transportation corridors due to limited mobility^[45]. Similarly, Chau *et al.* (2002) observed that reduced commuting needs among the elderly in Hong Kong contribute to lower traffic-related exposure^[48]. However, such conclusions should be interpreted with caution, as they may overlook the impact of residential pollution distribution. If elderly populations are concentrated in older urban areas or near industrial zones, their static exposure risk could be underestimated.

In summary, the weekend effect and the exposure characteristics of the elderly observed in this study align with findings from various global regions. However, the complexity of gender-based exposure differences underscores the need to account for regional cultural contexts (e.g., occupational roles and family responsibilities) and exposure pathways (i.e., the interplay between occupational and indoor microenvironment exposures). Future research could benefit from integrating high-resolution pollution data with individual behavioral trajectories (e.g., GPS-based activity patterns) to further reveal the mechanisms driving exposure disparities among population subgroups.

DISCUSSION

Spatiotemporal heterogeneity of conversion processes

The derived NO₂/NO_x ratio range (0.3-0.7), based on Luo Minghan's proportional simulation method, reflects the dynamic interplay between localized emission characteristics and atmospheric chemical processes in megacities such as Shanghai. This complexity is not adequately captured by national standard rates. Specifically:

Enhanced Photochemical Conversion: During summer in Shanghai, elevated temperatures, high relative humidity, and high solar radiation increase O₃ and VOC concentrations, which in turn promote the conversion of NO to NO₂^[50,51]. This process pushes the NO₂/NO_x ratio toward the upper limit (0.7).

Nonlinear Effects of Particulate Matter: During heavy pollution episodes, heterogeneous reactions on PM_{2.5}

surfaces, such as soot-catalyzed NO oxidation, further enhance NO₂ formation, contributing to an elevated ratio^[51].

Temporal Resolution Advantage: The national standard relies on annual averages, which overlook daily variations. Studies have shown that midday O₃ peaks can raise the NO₂/NO_x ratio to 0.6-0.7, while nighttime values drop to 0.3-0.4. These temporal patterns are supported by monitoring data^[52].

This broader ratio range more accurately captures the chemical complexity in high-emission, high-ozone urban environments, justifying its adoption for policy-relevant urban air quality modeling.

Group exposure disparities

This study reveals significant disparities in traffic-related NO₂ exposure across gender and age groups, highlighting the significance of activity-path-based environmental exposure assessment in environmental equity research.

Gender disparities

Gender-based differences in exposure to traffic pollution can be explained by the concept of the social stratification of road networks, as proposed by the Institute of Human Geography^[53]. Urban roads, as dynamic spaces of activity, serve both as infrastructure and public services, enabling access to various destinations. However, travel patterns differ substantially between genders due to factors such as family responsibilities, the division of labor, and environmental conditions, leading to gender-based segregation in mobility patterns and, ultimately, social stratification^[54].

Previous research has shown that women, who often bear the primary responsibility for household chores, tend to choose jobs located closer to home. Consequently, their daily mobility is subject to various limitations and constraints^[55]. As a result, women's travel typically involves short-distance, environmentally friendly trips, often along urban routes that include access to public transportation^[56]. In contrast, men generally have fewer domestic responsibilities and greater career mobility. Their longer commuting distances lead to a preference for high-capacity urban arterials and expressways to optimize travel efficiency.

Furthermore, the division of labor contributes to occupational disparities in traffic exposure. In Shanghai, men dominate employment in the transportation, warehousing, postal, and construction sectors. Specifically, men account for 72% of workers in transportation-related industries and as much as 83% in construction^[57]. Given these occupational trends and mobility behaviors, men experience greater exposure to traffic-related pollution and are therefore more vulnerable to its health impacts.

Age disparities

Significant differences in NO₂ exposure were also observed across age groups. Older adults experienced the lowest levels of exposure across all time periods, primarily due to their limited, short-distance, and temporally concentrated travel patterns. Their reliance on walking or cycling, along with a tendency to remain within community-based areas, further reduced their contact with high-pollution zones such as highways. In contrast, working-age adults (19-44 years), whose mobility is largely dictated by rigid commuting schedules and occupational demands, faced the highest NO₂ exposure, particularly during evening peak hours when pollutant concentrations exceeded daily averages.

These exposure disparities were most pronounced during the evening peak, likely due to the diversity of travel purposes and the wide dispersion of routes, which exacerbate inequities across age groups.

Compared to other age groups, older adults primarily engage in non-commuting travel, which is characterized by lower frequency, shorter distances, and briefer durations. On average, the elderly make 2.03 trips per day, slightly fewer than the 2.16 daily trips reported in Shanghai's Fifth Comprehensive Traffic Survey^[58]. Regarding travel distance and duration, juveniles, young adults, middle-aged adults, and older adults average 5.4, 7.7, 7.1, and 2.8 km per day, respectively. Corresponding average travel times are 24.4, 33.6, 31.7, and 16.2 min, respectively. Clearly, the elderly travel shorter distances and for less time than all other age groups.

Additionally, Huang *et al.* found that the elderly's activities are largely confined to their neighborhoods, with walking being the predominant mode of transport, supplemented by public transit and bicycles. When feasible, approximately 80% of seniors prioritize walking^[59]. This pattern results in a strong preference for low-grade roads, such as neighborhood and branch roads, and minimal use of expressways and arterial roads. As a result, the elderly group is exposed to significantly lower levels of traffic-related pollution compared to other groups.

It is noteworthy that the greatest disparity in exposure risk among age groups occurs during evening peak hours, with a maximum difference of 2.88 $\mu\text{g}/\text{m}^3$, followed by daytime (up to 2.27 $\mu\text{g}/\text{m}^3$). Differences during the morning peak and nighttime are relatively smaller, at 1.37 and 1.25 $\mu\text{g}/\text{m}^3$ respectively. These variations align with age-specific travel behavior. For instance, older adults demonstrate a reverse parabolic pattern in travel intensity - peaking during the morning and evening and tapering off in the afternoon^[60].

Uncertainty analysis

This study integrates the CALPUFF dispersion model with dynamic mobile phone signaling data to enhance the spatiotemporal resolution of exposure assessments. However, several sources of uncertainty remain and warrant further refinement:

(1) Data Representativeness and Sampling Bias

Although the spatial distribution, gender, and age structure of the mobile phone signaling data are broadly consistent with the Seventh National Population Census, the sample covers only 23.5% of the city's population. This may lead to underrepresentation of low-mobility groups (e.g., older adults or children). Furthermore, the inference-based classification of gender and age may introduce additional errors.

(2) Uncertainty in NO_2 Concentration Estimation

NO_2 concentrations are estimated from NO_x emissions using hourly NO_2/NO_x conversion rates (range: 0.3-0.7), which improves the temporal accuracy compared to fixed conversion factors. While this approach better captures diurnal pollution variations, it remains influenced by meteorological conditions and photochemical processes, potentially overlooking short-term spikes or atypical weather patterns.

(3) Regional Limitations

This study focuses on Baoshan District, an industrial area on the outskirts of Shanghai characterized by freight-intensive transportation, which may limit the generalizability of the findings to central urban areas or non-port cities. Nevertheless, the proposed methodology is highly transferable and offers a replicable framework for application in other regions.

(4) Temporal Resolution Constraints

While hourly simulations effectively capture broad trends in dynamic exposure, they lack the resolution needed to detect minute-level pollution peaks, such as those occurring in traffic-congested areas. Future work could incorporate higher-frequency trajectory data and real-time monitoring to refine exposure modeling.

CONCLUSIONS

Key findings

This study, using Shanghai's Baoshan District as a case study, developed a dynamic exposure risk assessment framework by integrating the CALPUFF dispersion model with mobile phone signaling data, systematically revealing the spatiotemporal distribution patterns and demographic disparities associated with traffic-related NO₂ pollution. The key findings include:

Temporal Dimension: NO₂ exposure exhibited a clear bimodal diurnal pattern, with noticeable weekday-weekend variations. Concentrations peaked during the morning and evening rush hours, while weekend levels remained consistently lower. This “rhythmic” pattern highlights the strong correlation between traffic emissions and human activity, providing a quantitative basis for “time-targeted pollution control”.

Spatial Dimension: Areas of high exposure risk clustered around ports, logistics corridors, and the outer-ring expressways, forming a spatial distribution pattern closely tied to the city's functional zoning. This spatial correlation suggests that uneven transportation infrastructure may contribute to environmental inequities.

Demographic Dimension: Exposure risks varied significantly by gender and age group. Males and working-age adults (19-44 years) experienced the highest exposure risks, whereas older adults faced the lowest risks due to their infrequent and short-distance travel behavior. These disparities reflect differences in mobility patterns and highlight the “social-behavioral and structural” nature of traffic pollution exposure.

Policy implications

Time-based traffic management strategies

Traffic-related NO₂ exposure peaks during morning and evening rush hours, especially when freight and commuter traffic overlap (e.g., during the evening peak). This overlap results in elevated NO₂ concentrations and higher exposure levels for local residents. To address this, dynamic traffic management strategies should be implemented to reduce pollutant loads during critical time windows. For example, staggered commuting schedules and time-specific restrictions on heavy-duty diesel trucks should be enforced during weekday peak hours, particularly in densely populated areas along major transport corridors such as the Outer Ring Expressway. Diverting freight traffic away from peak residential travel times can help reduce cumulative emissions, flatten intra-day pollution peaks, and limit short-term NO₂ buildup.

Targeted protection for high-exposure populations

Exposure assessments reveal that highly mobile groups, particularly working-age males, are disproportionately affected by traffic-related NO₂ pollution, while elderly individuals - due to their limited mobility - experience the lowest exposure. To address this disparity, targeted interventions should prioritize high-exposure populations to reduce health risks and promote environmental equity. For example, individuals with frequent commutes and high exposure levels should benefit from tailored protective

measures. Simulation results highlight persistently high NO₂ concentrations along key corridors in the southern part of Baoshan District, such as Baoyang Road and the Outer Ring Expressway near the port area. Installing air purification systems and vegetative buffers along these heavily trafficked routes could help reduce inhalation risks for passersby. Additionally, promoting flexible work arrangements can lower exposure during peak hours, and enhanced occupational safety guidelines should be established for outdoor workers in high-exposure zones. These tailored strategies can significantly reduce risks for working-age individuals while also accommodating the needs of more vulnerable groups, thereby strengthening population-wide resilience to air pollution.

Spatial optimization of high-risk zones

Modeling results identify specific high-risk zones in the southern part of Baoshan District where traffic-related pollution exposure is spatially concentrated. These areas often serve dual roles as transportation hubs (e.g., ports, logistics parks, and expressway intersections) and high-density residential communities, compounding exposure risks. To mitigate these effects, spatial planning and environmental regulation should be employed to optimize land use. On one hand, green infrastructure should be expanded in high-pollution areas, such as logistics corridors and port-adjacent neighborhoods. For example, establishing vegetation barriers along Baoyang Road and the Outer Ring Expressway can help intercept and dilute vehicle emissions before they reach residential areas. On the other hand, land use and functional zoning policies should be refined to reduce the co-location of emission-intensive roads with sensitive land uses such as housing, schools, and hospitals. Strategic urban planning that spatially decouples residential areas from high-emission corridors will be key to lowering long-term exposure levels and addressing spatial inequities in environmental health outcomes.

Limitations

Limited Spatial Applicability: This study focuses on Baoshan, an industrial logistics-oriented district, which may limit the applicability of the findings to urban cores or non-port cities.

Data Constraints: The analysis relies on mobile signaling data to infer group attributes and movement trajectories, which may lack precision. More granular data sources (e.g., travel diaries or wearable devices) are needed to enhance accuracy.

Unquantified Health Impacts: While the study assesses exposure levels, it does not directly model the causal links between exposure and health outcomes.

DECLARATIONS

Acknowledgments

The authors express gratitude to all those who have provided assistance during the writing of this thesis.

Authors' contributions

Conceptualization, formal analysis: Wang, S.; Luo, X.; Liu, C.

Software: Wang, H.; Wang, Q.; Fu, Y.

Investigation, resources: Fu, Q.; M.Y.

Data curation: Fu, Q.; Guo, X.; Yi, M.

writing - review and editing: Wang, S.; Fu, Y.; Luo, X.; Liu, C.

Supervision: Luo, X.; Liu, C.

Visualization: Wang, H.

Methodology, writing - original draft, validation: Wang, S.

Project administration, funding acquisition: Luo, X.

All authors have read and approved the published version of the manuscript.

Availability of data and materials

The data presented in this study are available from the corresponding authors upon reasonable request. The data are not publicly available due to privacy restrictions.

Financial support and sponsorship

This research was sponsored by the General Project of NSFC (No.52372340) and the International Cooperation and Exchanges NSFC (No.72061137071).

Conflicts of interest

Dr. Luo, X. is the Guest Editor of the Special Issue “Challenges and Opportunities for Transport Carbon Neutrality”. Dr. Luo was not involved in any steps of the editorial processing of this manuscript, including reviewer selection, manuscript handling, or decision making. The funders had no role in the design of the study; in the collection, analyses, or interpretation of data; in the writing of the manuscript; or in the decision to publish the results, while the other authors have declared that they have no conflicts of interest.

Ethical approval and consent to participate

Not applicable.

Consent for Publication

Not applicable.

Consent for publication

© The Author(s) 2025.

REFERENCES

1. Ministry of Ecology and Environment of China. State of the ecological environment bulletin. 2020. Available from: <https://www.mee.gov.cn/hjzl/sthjzk/zghjzkqgb/> [Last accessed on 19 May 2025].
2. Anenberg, S. C.; Mohegh, A.; Goldberg, D. L.; et al. Long-term trends in urban NO₂ concentrations and associated paediatric asthma incidence: estimates from global datasets. *Lancet. Planet. Health.* **2022**, *6*, e49-58. DOI
3. Ott, W. R. Concepts of human exposure to air pollution. *Environ. Int.* **1982**, *7*, 179-96. DOI
4. Smith, K. R. Air pollution assessing total exposure in the United States. *Environ. Sci. Policy. Sustain. Dev.* **1988**, *30*, 10-38. DOI
5. Afzali, A.; Rashid, M.; Afzali, M.; Younesi, V. Prediction of air pollutants concentrations from multiple sources using AERMOD coupled with WRF prognostic model. *J. Clean. Prod.* **2017**, *166*, 1216-25. DOI
6. Claggett, M. Comparing predictions from the CAL3QHCR and AERMOD models for highway applications. *Transport. Res. Rec.* **2014**, *2428*, 18-26. DOI
7. Carruthers, D.; Holroyd, R.; Hunt, J.; et al. UK-ADMS: a new approach to modelling dispersion in the earth's atmospheric boundary layer. *J. Wind. Eng. Ind. Aerod.* **1994**, *52*, 139-53. DOI
8. Scire, J. S.; Strimaitis, D. G.; Yamartino, R. J. A user's guide for the CALPUFF dispersion model. Concord, MA: Earth Tech Inc., 2000. Available from: https://www.eoas.ubc.ca/courses/atsc507/ADM/calpuff/documentation/CAL-v5/CALPUFF_UsersGuide.pdf [Last accessed on 19 May 2025].
9. Ghannam, K.; El-Fadel, M. Emissions characterization and regulatory compliance at an industrial complex: an integrated MM5/CALPUFF approach. *Atmos. Environ.* **2013**, *69*, 156-69. DOI
10. Ergun, P.; Kara, M.; Bayram, A.; Dumanoglu, Y.; Altioek, H.; Elbir, T. Application of an activity based approach to assess air quality from mobile sources in an urban center. *Curr. Environ. Eng.* **2014**, *1*, 64-72. DOI
11. Joo, S.; Oh, C.; Lee, S.; Lee, G. Assessing the impact of traffic crashes on near freeway air quality. *Transp. Res. Part. D.* **2017**, *57*, 64-73. DOI
12. Charabi, Y.; Abdul-Wahab, S.; Al-Rawas, G.; Al-Wardy, M.; Fadlallah, S. Investigating the impact of monsoon season on the dispersion of pollutants emitted from vehicles: a case study of Salalah city, sultanate of Oman. *Transp. Res. Part. D.* **2018**, *59*, 108-20. DOI

13. Abdul-Wahab, S. A.; Fadlallah, S. O. A study of the effects of vehicle emissions on the atmosphere of Sultan Qaboos University in Oman. *Atmos. Environ.* **2014**, *98*, 158-67. DOI
14. Broomandi, P. Modeling of air pollutants' dispersion by means of CALMET/CALPUFF (case study: district 7 in Tehran city). 2018. DOI
15. Farrell, W.; Weichenthal, S.; Goldberg, M.; Valois, M. F.; Shekarzifard, M.; Hatzopoulou, M. Near roadway air pollution across a spatially extensive road and cycling network. *Environ. Pollut.* **2016**, *212*, 498-507. DOI PubMed
16. Zhang, Y.; Cai, M.; Wang, Z. Study on the distribution characteristics of PM_{2.5} on both sides of the elevated road in Guangzhou. *Transp. Energy. Conserv. Environ. Prot.* **2019**, *15*, 76-81. DOI
17. Shekarzifard, M.; Faghih-Imani, A.; Hatzopoulou, M. An examination of population exposure to traffic related air pollution: comparing spatially and temporally resolved estimates against long-term average exposures at the home location. *Environ. Res.* **2016**, *147*, 435-44. DOI PubMed
18. Chen, Y.; Ebenstein, A.; Greenstone, M.; Li, H. Evidence on the impact of sustained exposure to air pollution on life expectancy from China's Huai River policy. *Proc. Natl. Acad. Sci. USA.* **2013**, *110*, 12936-41. DOI PubMed PMC
19. Fabisiak, J. P.; Jackson, E. M.; Brink, L. L.; Presto, A. A. A risk-based model to assess environmental justice and coronary heart disease burden from traffic-related air pollutants. *Environ. Health.* **2020**, *19*, 34. DOI PubMed PMC
20. Levy, I.; Karakis, I.; Berman, T.; Amitay, M.; Barnett-Itzhaki, Z. A hybrid model for evaluating exposure of the general population in Israel to air pollutants. *Environ. Monit. Assess.* **2019**, *192*, 4. DOI PubMed
21. Guo, H.; Yang, S.; He, X.; Qiao, B.; Li, M. Study on the exposure intensity of air pollution in Zhengzhou city based on nighttime lighting. *J. Henan. Polytech. Univ.* **2019**, *38*, 81-8. DOI
22. Zhang, X.; Hu, H. Risk assessment of exposure to PM_{2.5} in Beijing using multi-source data. *J. Peking. Univ.* **2018**, *54*, 1103-13. DOI
23. Lim, S.; Kim, J.; Kim, T.; et al. Personal exposures to PM_{2.5} and their relationships with microenvironmental concentrations. *Atmos. Environ.* **2012**, *47*, 407-12. DOI
24. Kousa, A.; Oglesby, L.; Koistinen, K.; Künzli, N.; Jantunen, M. Exposure chain of urban air PM_{2.5} - associations between ambient fixed site, residential outdoor, indoor, workplace and personal exposures in four European cities in the EXPOLIS-study. *Atmos. Environ.* **2002**, *36*, 3031-9. DOI
25. Fu, Q.; Kan, H. Air pollution dispersion model and assessment of population weighted exposure. *J. Environ. Health.* **2004**, 414-6. DOI
26. Hoek, G.; Brunekreef, B.; Goldbohm, S.; Fischer, P.; van, B. P. A. Association between mortality and indicators of traffic-related air pollution in the Netherlands: a cohort study. *Lancet* **2002**, *360*, 1203-9. DOI PubMed
27. Zou, B.; Pu, Q.; Luo, Y.; Tian, Y.; Zhang, W. Research on multi-indicator spatial zoning for urban PM_{2.5} pollution prevention and control. *J. Saf. Environ.* **2016**, *16*, 337-42. DOI
28. Saraswat, A.; Kandlikar, M.; Brauer, M.; Srivastava, A. PM_{2.5} population exposure in New Delhi using a probabilistic simulation framework. *Environ. Sci. Technol.* **2016**, *50*, 3174-83. DOI
29. Tang, R.; Tian, L.; Thach, T. Q.; et al. Integrating travel behavior with land use regression to estimate dynamic air pollution exposure in Hong Kong. *Environ. Int.* **2018**, *113*, 100-8. DOI
30. Brusselaers, N.; Macharis, C.; Mommens, K. The health impact of freight transport-related air pollution on vulnerable population groups. *Environ. Pollut.* **2023**, *329*, 121555. DOI PubMed
31. Xu, Y.; Yi, L.; Cabison, J.; et al. The impact of GPS-derived activity spaces on personal PM_{2.5} exposures in the MADRES cohort. *Environ. Res.* **2022**, *214*, 114029. DOI PubMed PMC
32. Guo, H.; Li, W.; Yao, F.; et al. Who are more exposed to PM_{2.5} pollution: a mobile phone data approach. *Environ. Int.* **2020**, *143*, 105821. DOI
33. Lu, Y.; Habre, R. Impacts of distinct travel behaviors on potential air pollution exposure measurement error. *Atmos. Environ.* **2023**, *306*, 119820. DOI
34. Cutter, S. L. Race, class and environmental justice. *Prog. Human. Geogr.* **1995**, *19*, 111-22. DOI
35. Martuzzi, M.; Mitis, F.; Forastiere, F. Inequalities, inequities, environmental justice in waste management and health. *Eur. J. Public. Health.* **2010**, *20*, 21-6. DOI PubMed
36. Mitchell, G.; Norman, P.; Mullin, K. Who benefits from environmental policy? An environmental justice analysis of air quality change in Britain, 2001-2011. *Environ. Res. Lett.* **2015**, *10*, 105009. DOI
37. Ministry of Ecology and Environment of China. Technical guidelines for environmental impact assessment - atmospheric environment. 2018. Available from: https://www.mee.gov.cn/ywggz/fgbz/bz/bzwb/other/pjjsdz/201808/t20180814_451386.shtml [Last accessed on 19 May 2025].
38. Luo, M.; Ding, T.; Chen, Q. Characteristics and simulation methods for photochemical transformation of nitrogen oxides. *Environ. Eng.* **2017**, *35*, 106-12. DOI
39. Wang, H.; Luo, X.; Liu, C.; Fu, Q.; Yi, M. Spatio-temporal variation-induced group disparity of intra-urban NO₂ exposure. *Int. J. Environ. Res. Public. Health.* **2022**, *19*, 5872. DOI PubMed PMC
40. Ta, N.; Wang, X.; Hu, L.; Liu, Z. Gender difference in commuting travel: a comparative study of suburban residents in Beijing and Shanghai. *Transp. Policy.* **2022**, *28*, 196-203. DOI
41. Ministry of Ecology and Environment of China. Shanghai's air pollution control efforts found lacking. Available from: https://www.mee.gov.cn/ywggz/zyshjbhdc/dclj/202406/t20240613_1075708.shtml [Last accessed on 19 May 2025].

42. Feng, J.; Yang, Z. Factors influencing travel behavior of urban elderly people in Nanjing. *J. Transp. Geogr.* **2015**, *34*, 1598-608. DOI
43. Pommier, M. Estimations of NO_x emissions, NO₂ lifetime and their temporal variation over three British urbanised regions in 2019 using TROPOMI NO₂ observations. *Environ. Sci. Atmos.* **2023**, *3*, 408-21. DOI
44. Demetillo, M. A. G.; Harkins, C.; McDonald, B. C.; Chodrow, P. S.; Sun, K.; Pusede, S. E. Space-based observational constraints on NO₂ air pollution inequality from diesel traffic in major US cities. *Geophys. Res. Lett.* **2021**, *48*, e2021GL094333. DOI
45. Mo, S.; Wang, Y.; Peng, M.; et al. Sex disparity in cognitive aging related to later-life exposure to ambient air pollution. *Sci. Total. Environ.* **2023**, *886*, 163980. DOI
46. Hu, Y.; Yao, M.; Liu, Y.; Zhao, B. Personal exposure to ambient PM_{2.5}, PM₁₀, O₃, NO₂, and SO₂ for different populations in 31 Chinese provinces. *Environ. Int.* **2020**, *144*, 106018. DOI
47. Kim, H.; Noh, J.; Noh, Y.; Oh, S. S.; Koh, S. B.; Kim, C. Gender difference in the effects of outdoor air pollution on cognitive function among elderly in Korea. *Front. Public. Health.* **2019**, *7*, 375. DOI PubMed PMC
48. Chau, C. K.; Tu, E. Y.; Chan, D. W. T.; Burnett, J. Estimating the total exposure to air pollutants for different population age groups in Hong Kong. *Environ. Int.* **2002**, *27*, 617-30. DOI
49. Setton, E.; Keller, C. P.; Cloutier-Fisher, D.; et al. Gender differences in chronic exposure to traffic-related air pollution - A simulation study of working females and males. *Prof. Geogr.* **2010**, *62*, 66-83. DOI
50. Sillman, S. The relation between ozone, NO_x and hydrocarbons in urban and polluted rural environments. *Atmos. Environ.* **1999**, *33*, 1821-45. DOI
51. Atkinson, R. Atmospheric chemistry of VOCs and NO_x. *Atmos. Environ.* **2000**, *34*, 2063-101. DOI
52. Beidi, D. Temporal-spatial distribution characteristics of provincial industrial NO_x emissions and driving factors in China from 2006 to 2013. *Resour. Sci.* **2016**, *38*, 93-8. DOI
53. Chen, X. P.; Zhou, S. H.; Li, Q. P.; Zhan, W. Research on social differentiation of urban road network in Guangzhou: Gender differences of travel distribution based on trajectory data. *Geogr. Res.* **2021**, *40*, 1652-66. DOI
54. Shen, Y. Segregation through space: a scope of the flow-based spatial interaction model. *J. Transp. Geogr.* **2019**, *76*, 10-23. DOI
55. Kwan, M. P. Gender differences in space-time constraints. *Area* **2000**, *32*, 145-56. DOI
56. Tong, X.; Wang, Y. A gender comparative study of travel modes of urban residents. *J. Shanxi. Univ.* **2018**, *45*, 64-69. DOI
57. Shanghai Statistics Bureau. Analysis on the development status and characteristics of female population in Shanghai. 2011. Available from: <https://tjj.sh.gov.cn/tjfx/20111123/0014-236073.html> [Last accessed on 19 May 2025].
58. Institute of Urban and Rural Construction and Transportation Development. Main results of the fifth comprehensive traffic survey in Shanghai. *Traffic. Transp.* **2015**, *31*, 15-18. DOI
59. Huang, J.; Zhang, R.; Hu, G. Exploring the daily life circle of the elderly based on spatio-temporal behavior - Spatial recognition and feature analysis. *Urban. Plan. Forum.* **2019**, 87-95. DOI
60. Yan, H.; Jin, R.; Li, T. Research advancements in elderly travel behavior characteristics utilizing knowledge graphs. *J. Chang'an. Univ.* **2021**, *41*, 101-14. DOI